

## HEAT TRANSFER STUDY IN A VOLUMETRIC RECEIVER USED IN CONCENTRATING SOLAR POWER PLANTS

**Taísa Santos da Silva**, [taisa1106@hotmail.com](mailto:taisa1106@hotmail.com)

**Gabriel Cerqueira de Araújo**, [gabrielcerqueiradearaujo@gmail.com](mailto:gabrielcerqueiradearaujo@gmail.com)

**Fabio Santos Nascimento**, [fabiosn@unifei.edu.br](mailto:fabiosn@unifei.edu.br)

**Paulo Mohallem Guimarães**, [pauloguimaraes1961@gmail.com](mailto:pauloguimaraes1961@gmail.com)

Federal University of Itajubá - Itajubá Campus

Rua Irmã Ivone Drumond, 200, Distrito Industrial II, Itabira, Zip.: 35903-087, Brazil.

**Genésio J. Menon**,

Federal University of Itajubá - Itajubá Campus

Av. BPS, 1303, Bairro Pinheirinho, ZIP. 37500903, Brazil-

**Abstract.** *This is a numerical study on heat transfer in a volumetric receiver applied in solar plants based on concentrating solar radiation. The heliostat field concentrates solar radiation in the receiver at the top of a tower. The receiver consists of some parts named secondary concentrator, a window glass, an absorber media and an external pressurized vessel. The secondary concentrator focuses solar radiation into the glass window. The radiation goes through the window to the absorber porous media located inside the pressurized vessel. Absorber conducts heat to a heat transfer working fluid. In this work, this heat transfer agent is the air. Colder pressurized air enters the volumetric receiver inlet and exits through an outlet at higher temperatures. Then the hot air is used in some thermodynamic cycles to produce electricity. A simulation package is used to approximate solutions in order to improve thermal efficiency of the receiver considering a mixed convection heat transfer in steady-state regime. The mathematical model and the numerical techniques, which are used in this package, are validated with some benchmark problems found in literature. However, only one is shown here. The result is for a dimensional study with a high temperature imposed on the porous media surface. It is observed that the porous media strongly plays its role as to increase the contact area of air to be heated and the solid conductive material with prescribed temperature on one surface as to approximate effects of incident radiation on such surface. Radiation is not considered in this work.*

**Keywords:** *Concentrating Solar Plant, Volumetric Receiver, Heat transfer, Solar Power Tower.*

### 1. INTRODUCTION

Clean and renewable energy generation is among the most discussed topics by the scientific community, due to the drawbacks of traditional source (fossil fuel) and the world energy consumption increase. Concentrated solar power (CSP) is a clean generation that has gained major focus of research over the last fifty years. The main source of CSP is the more abundant energy in the environment, the sun. There are four technology types: Parabolic, Dish, Central Tower and Fresnel. Central tower power plants with volumetric concentrator have shown high performance in the production of clean and cheap energy.

A study by Behar (2013) analyzed researches related to solar thermal power plants with central receiver, indicating that systems with volumetric receiver technology have great energy potential. In turn, Avila-Martin (2011) reviewed types of volumetric receivers, indicating the receiver from REFOS program as the most efficient. Albanakis (2009) studied types of porous materials which have better performances in thermal energy convection to the system fluid.

The study of Buck (2001) demonstrated that plants using volumetric central receiver has the potential to compete in today's market. In 2031, one system with central volumetric receiver was built by Del Río. Currently, It is on the first test phase using part of the solar field of Solugas. Later, this innovation will be applied to the Abengoa plant, allowing its entry into the market and reducing the cost of energy.

### 2. RECEIVER DESIGN AND PROBLEM FORMULATION

The problem to be studied consists of a volumetric receiver, considering steady laminar forced convection. This first analysis takes into consideration air as the working fluid and Silicon Carbide as the solid material in the porous media matrix. Figure 1 depicts the geometry and the boundary conditions of the problem. The computational domain consists of four subdomains that are signalized by the squares in Figure 1. These subdomains are the air domain (regions 1, 2 and 3) and the porous media domain (region 4). Table 1 shows the properties of Silicon Carbide and air, respectively. The boundary conditions are shown by the circles which are related to the surfaces they are in contact with.

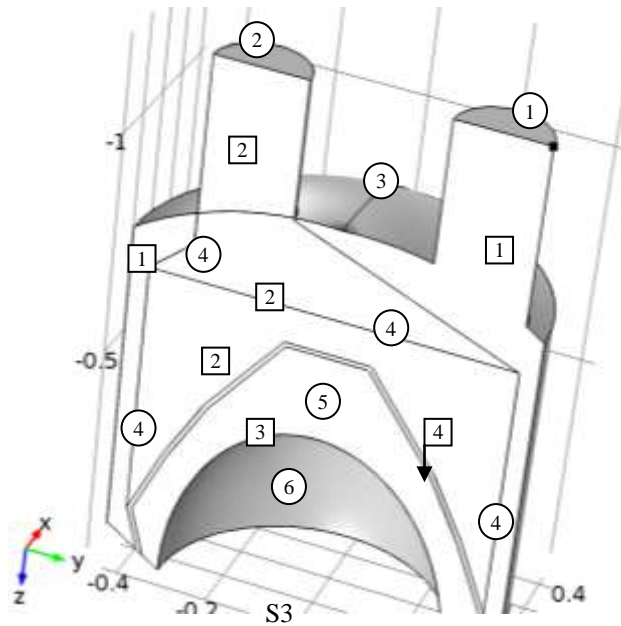


Figure 1. Geometry and boundary conditions.

Surface 1: inlet: Inflow velocity ( $V_0$ ): 0.5 m/s, temperature ( $T_0$ ): 293.15 K;  $p_0 = 15$  bar.

Surface 2: outlet: developed flow conditions.

Surface 3, 4 and 6: outer walls: no-slip condition, thermal isolation.

Surface 5: temperature: ( $T_{\text{matrix}}$ ) 800 K.

All surfaces belonging to the cut plane are under symmetry conditions (flow and heat symmetry).

Table 1. Properties of Silicon Carbide.

Name	Value	Unit
Heat capacity at constant pressure	900[J/(kg*K)]	J/(kg*K)
Density	3100[kg/m <sup>3</sup> ]	kg/m <sup>3</sup>
Thermal conductivity	150[W/(m*K)]	W/(m*K)
Permeability	0.0001	m <sup>2</sup>
Ratio of specific heats	1	1
Dynamic viscosity	1	Pa*s
Young's modulus	300e9[Pa]	
Poisson's ratio	0.14	

On the surfaces interfacing two different domains, appropriate boundary conditions are imposed in relation to one another. The governing equations for such a problem are:

1. For the fluid domain:

The mass conservation equation:

$$\nabla \cdot (\rho \mathbf{u}) = 0 \quad (1)$$

The momentum conservation equation:

$$\rho (\mathbf{u} \cdot \nabla) \mathbf{u} = \nabla \cdot \left[ -p \mathbf{I} + \mu (\nabla \mathbf{u}) + (\nabla \mathbf{u})^T - \frac{2}{3} \mu (\nabla \mathbf{u}) \mathbf{I} \right] \quad (2)$$

The energy conservation equation:

$$\rho C_p \mathbf{u} \cdot \nabla T = \nabla \cdot (k \nabla T) \quad (3)$$

where  $\mathbf{u}$  is the fluid velocity vector,  $\rho$  is the fluid density,  $\mathbf{I}$  is the identity vector,  $\mu$  is the dynamic viscosity,  $C_p$  is the specific heat,  $k$  is the fluid thermal conductivity,  $p$  is the pressure and  $T$  is the temperature.

2. For the porous matrix (Brinkman's equations)

$$\frac{\rho}{\varepsilon_p} \left( \mathbf{u} \cdot \nabla \right) \frac{\mathbf{u}}{\varepsilon_p} = \nabla \cdot \left[ -p\mathbf{I} + \frac{\mu}{\varepsilon_p} (\nabla \mathbf{u} + (\nabla \mathbf{u})^T) - \frac{2\mu}{3\varepsilon_p} (\nabla \cdot \mathbf{u}) \mathbf{I} \right] - \left( \mu K^{-1} + \beta_F |\mathbf{u}| + \frac{Q_{br}}{\varepsilon_p^2} \right) \mathbf{u} \quad (4)$$

$$\rho \nabla \cdot \mathbf{u} = Q_{br} \quad (5)$$

where  $\varepsilon_p$  is porosity and  $K$  is the permeability.

### 3. Heat transfer in porous media

$$\rho C_p \mathbf{u} \nabla T = \nabla \cdot (k_{eq} \nabla T) \quad (6)$$

$$k_{eq} = \theta_p k_p + (1 - \theta_p) k \quad (7)$$

where  $\theta_p$  is the volume fraction,  $k_p$  is the effective thermal conductivity fluid of the fluid-solid mixture.

### 3. VALIDATION

One of the validations was the porous media problem whose results were contrasted with the ones by Hossain and Wilson (2002). It is a study of natural convection in a square cavity containing porous medium.  $T_c$  is the temperature on the cold surfaces and  $T_h$  is the temperature on the heated surfaces. There is a region on the bottom right vertical wall where the temperature varies linearly. This validation can be found in the COMSOL documentations. Temperature and velocities behaviors are contrasted. There is an excellent agreement.

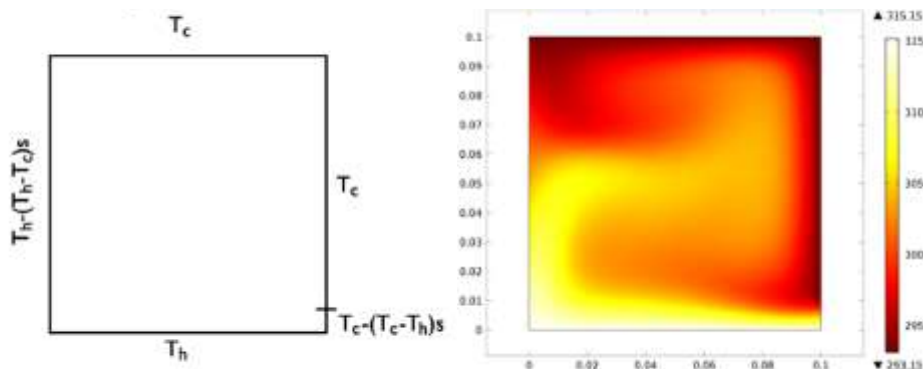


Figure 2. Geometry, boundary conditions and the isotherms for Rayleigh number equal to  $10^5$ .

### 4. NUMERICAL METHOD

The COMSOL Multiphysics was used to approximate solutions to the governing equations. The finite element method is used. Figure 3 shows the mesh used and table 2 shows the mesh statistics.

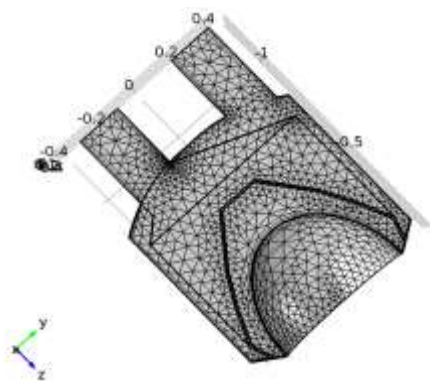


Figure 3. Mesh with tetrahedral elements.

Table 2. Mesh statistics.

Property	Value
Minimum element quality	0.007453
Average element quality	0.5319
Tetrahedral elements	46403
Pyramid elements	1012
Prism elements	10496
Triangular elements	9810
Quadrilateral elements	428
Edge elements	975
Vertex elements	61

## 5. RESULTS

Figure 4 shows the thermal field of the four domains: a) entrance region, b) exit region, c) intermediate region and d) the porous region for  $V_0 = 0.5$  m/s,  $T_0 = 293.15$ K,  $T_{\text{matrix}} = 800$ K and  $p_0 = 15$  bar. The entrance region (a) temperature varies from 293 to 800k. This more heated region is placed on the lower region that is in contact with the porous region surface that is at 800 K. Air is significantly heated as it passes through the porous region. In the exit region (b), that is the region after the porous matrix, temperature ranges from 621K to 796K. It is worth seeing that the coldest place in this region is in its lower part. There was about a 273% temperature increase when comparing to the inlet air temperature of 293.15K. This is due to the porous medium effect that plays a role of augmenting the thermal contact between air and the porous material. Region (c) presents almost a uniform temperature of 800K. The thickness of this porous layer is small and the solid material used with moderate thermal conductivity ( $k = 27$  W/mK). An interesting study here is to optimize the thickness of this porous matrix in order to achieve the best heat transfer possible taking into consideration pressure load gained and material cost.

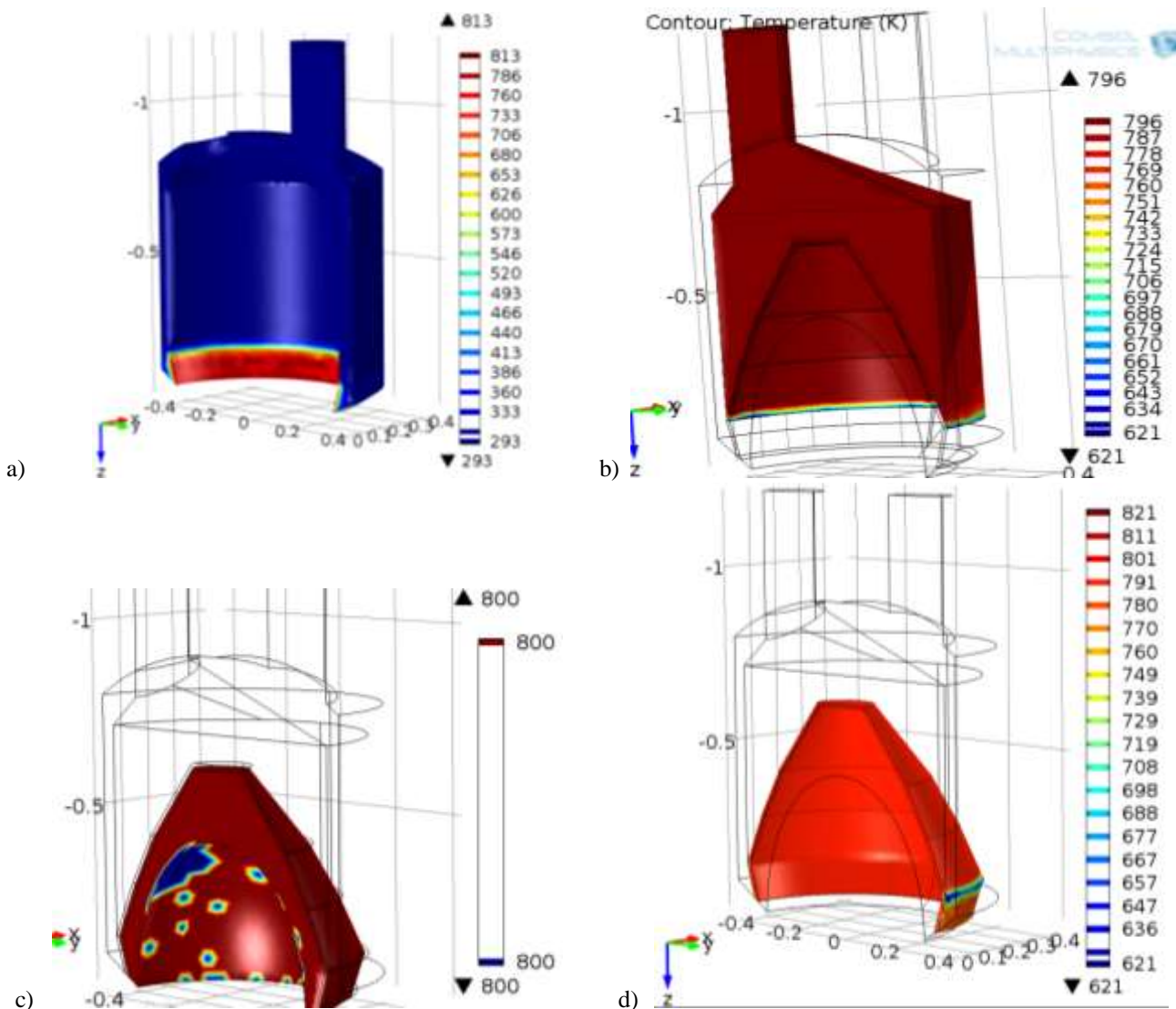


Figure 4. Isotherms for the four domains  
 ( $V_0 = 0.5$  m/s,  $T_0 = 293.15$ K,  $T_{\text{matrix}} = 800$ K and  $p_0 = 15$  bar)

Figure 5 shows the streamlines for the case from Fig. 4. For a velocity entrance of 0.5 m/s, the flow field seems to be organized with no significant recirculations. One can observe the air passing through the porous media. This geometry assures that the air (red lines) moves from the entrance tube and then flows over the internal chamber and then reaches the lower porous media inlet. It seems to be interesting to analyse the velocity field to check if air flow is uniform on the porous media inlet.

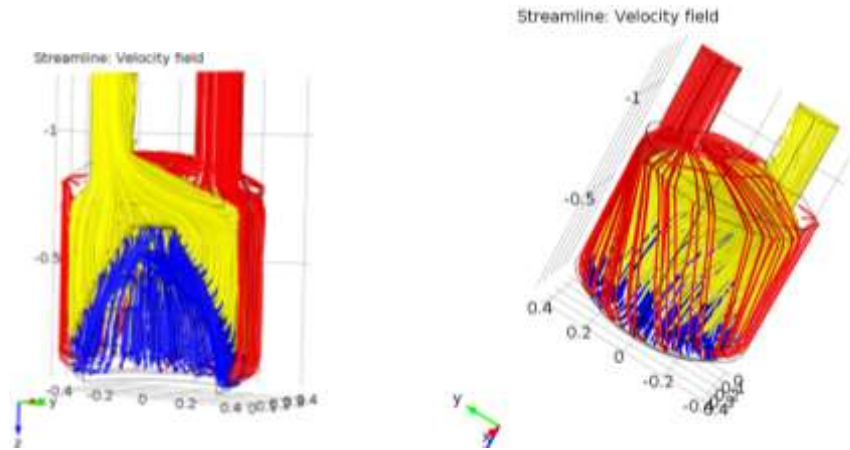


Figure 5. Streamlines  
 ( $V_0 = 0.5 \text{ m/s}$ ,  $T_0 = 293.15\text{K}$ ,  $T_{\text{matrix}} = 800\text{K}$  and  $p_0 = 15 \text{ bar}$ )

Figure 6 presents the velocity field for the four domains for the case from Fig. 4. For the porosity of 0.4, the exit velocity is almost four times bigger than the entrance velocity, although the tubes have the same diameter. It is interesting to analyse in future works the air compressibility for this kind of systems. In this test case, air is considered incompressible. As expected, the velocities in the porous media are lower. Due to the incompressibility effect, higher velocity regions have lower pressure fields (see Figure 7). One point that must be taken into consideration for future studies is the high pressure difference in the porous matrix. Silicone Carbide is being used in the porous matrix as due to it supports great pressure differences, thermal shock and water hammers caused by turning on and off of turbines in the net.

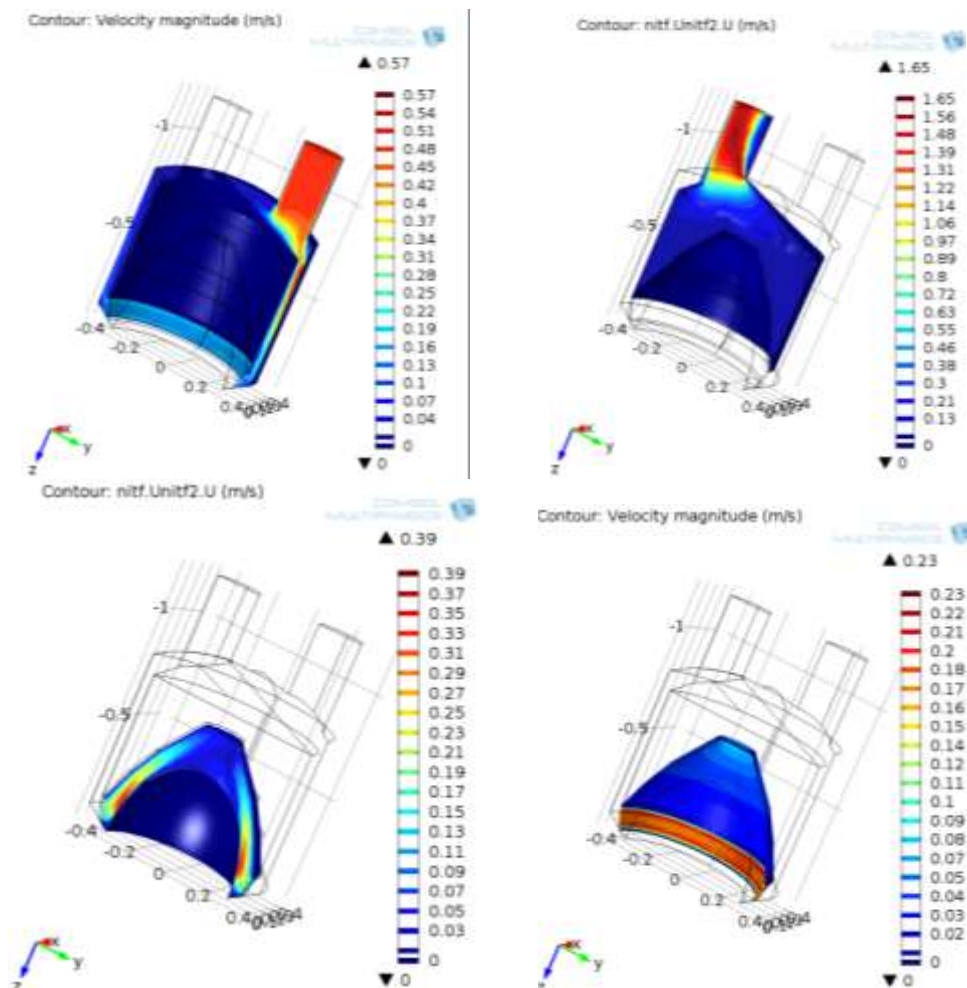


Figure 6. Velocity field  
 ( $V_0 = 0.5 \text{ m/s}$ ,  $T_0 = 293.15\text{K}$ ,  $T_{\text{matrix}} = 800\text{K}$  and  $p_0 = 15 \text{ bar}$ )

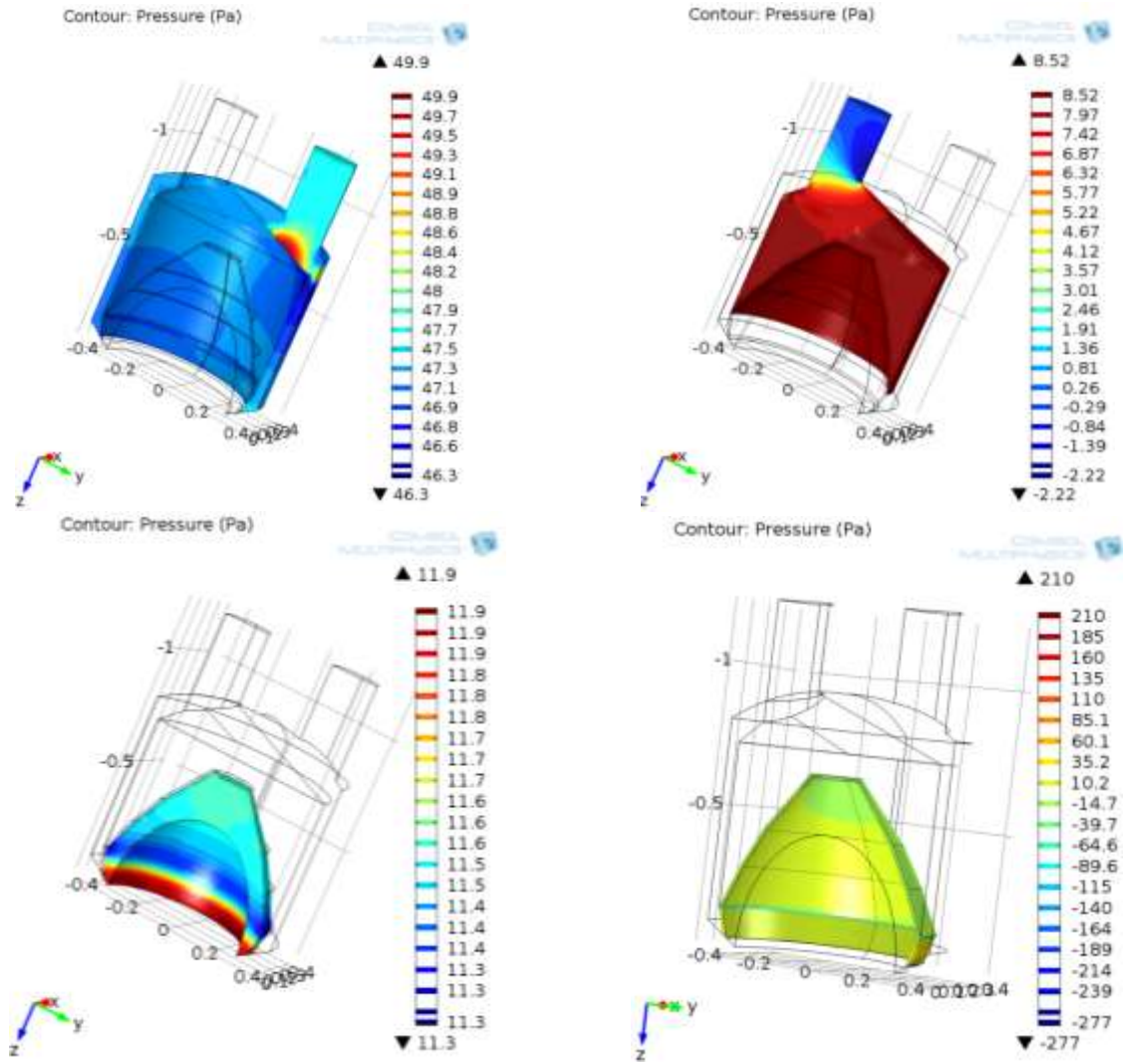
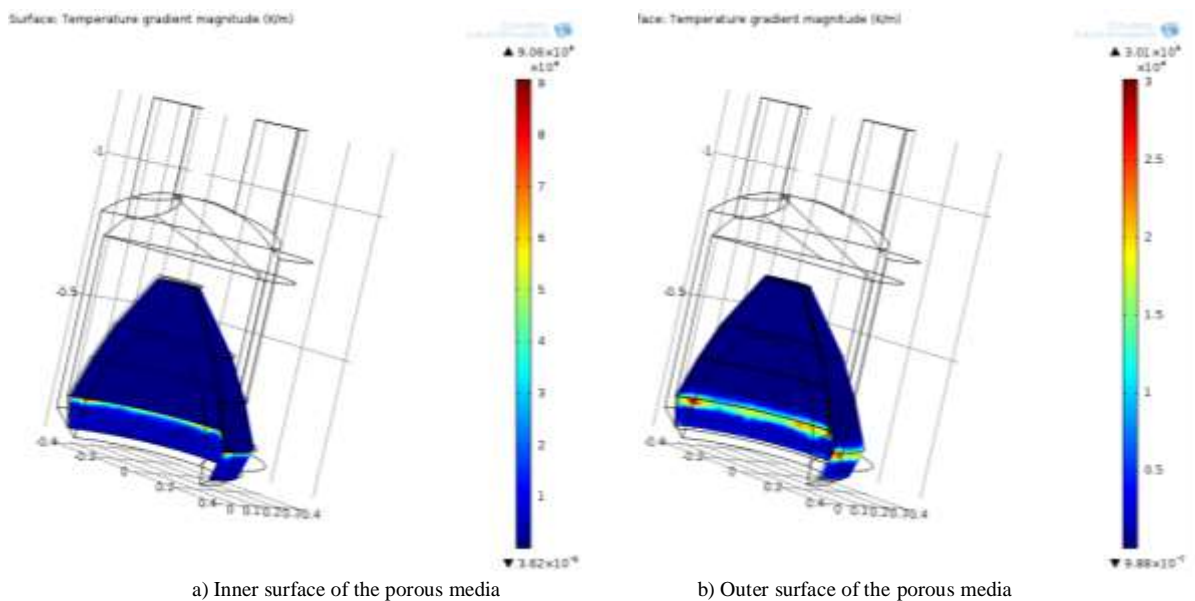


Figure 7. Pressure field ( $V_0 = 0.5 \text{ m/s}$ ,  $T_0 = 293.15\text{K}$ ,  $T_{\text{matrix}} = 800\text{K}$  and  $p_0 = 15 \text{ bar}$ )



a) Inner surface of the porous media

b) Outer surface of the porous media

Figure 8. Temperature gradients of the inner and outer surfaces of the porous media  
 ( $V_0 = 0.5 \text{ m/s}$ ,  $T_0 = 293.15\text{K}$ ,  $T_{\text{matrix}} = 800\text{K}$  and  $p_0 = 15 \text{ bar}$ )

In Fig. 8, one can see the behavior of the temperature gradients of the porous material on its inner and outer surfaces. Just in accordance with the temperature field, there are greater gradients near the upper part of the lower entrance region. Figure 9 also depicts the gradient temperatures inside the porous media.

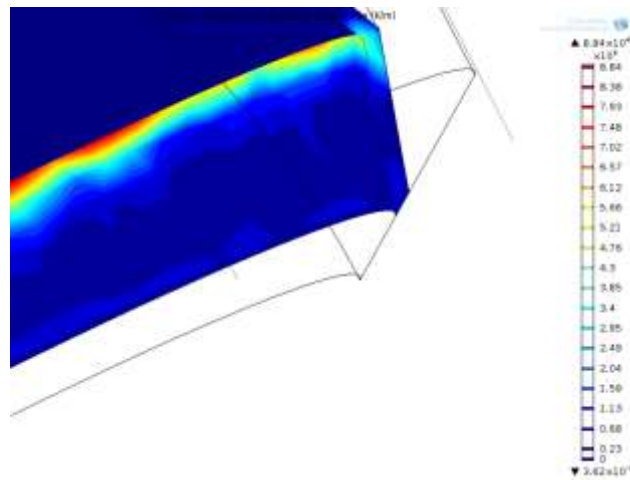


Figure 9. Temperature gradients of the porous media  
 ( $V_0 = 0.5 \text{ m/s}$ ,  $T_0 = 293.15\text{K}$ ,  $T_{\text{matrix}} = 800\text{K}$  and  $p_0 = 15 \text{ bar}$ )

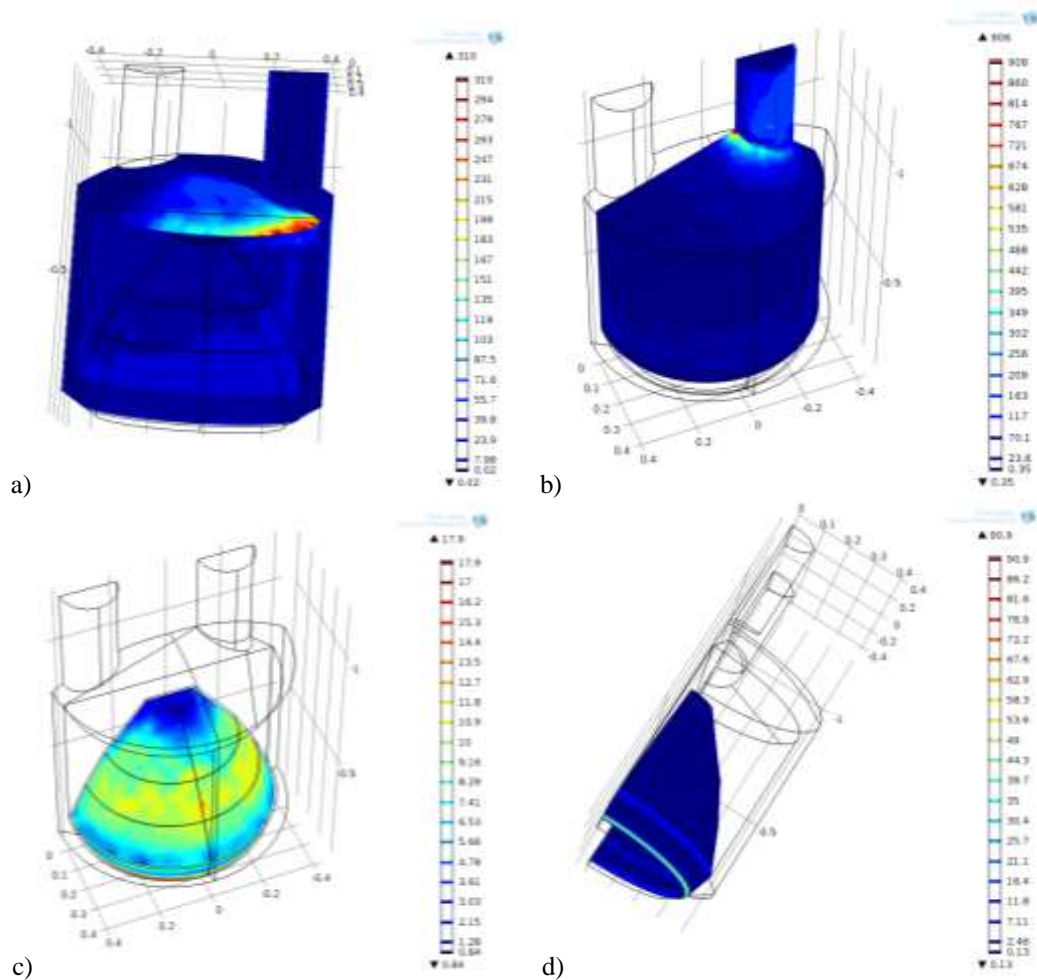


Figure 10. Shear rate behavior.

Figure 10 shows the shear rate in the entrance domain (a), the exit domain (b), the intermediate domain (c) and the porous matrix domain. Shear rate is the rate at which a progressive shearing deformation is applied to some material or

to the walls. As expected, borders are likely to have higher shear stresses. One may note that in the shear stress is not related to the field with highest pressure. For instance, the domain with highest average shear stress is the exit domain whereas the region that presents the highest average pressure field is the porous media. However, the field that shows the highest is the one with higher average temperatures.

Finally, Fig. 11 depicts the conductive and convective heat fluxes in the porous media. Heat convection is clearly higher in the bottom of the matrix. When the fluid passes through the bottom, this region is already heated and then the fluid passes through the porous matrix again, to find its path to the exit region.

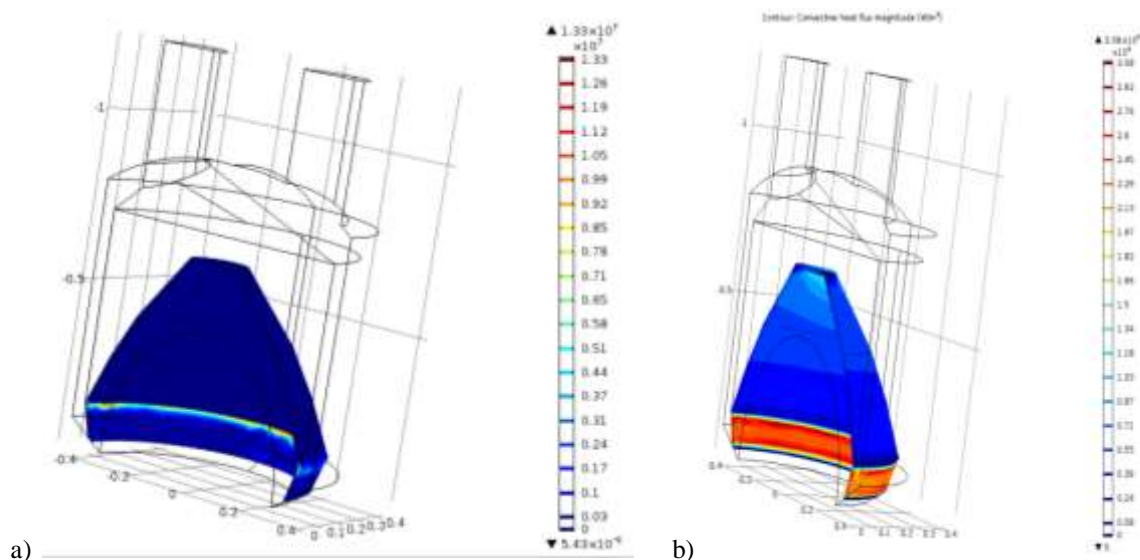


Figure 11. Conductive (a) and convective (b) heat fluxes in the porous media.

## 6. CONCLUSION

This work studies the mixed convection heat transfer in a laminar regime inside a volumetric receiver used in concentrating solar power plants. Although this is a subject already developed in some countries such as Spain, Germany, USA, Brazil does not have its plant yet. That is why it is so important to stimulate students and teachers on this field. It is a promising clean energy source that can be successfully implemented in Rankine and Brayton cycles, for instance. Therefore, the main contribution of this work is to learn the physics and a mathematical model that be used in this problem and the basic temperature, velocity, and pressure behaviors of the work fluid. Air is significantly heated as it passes through the porous region. In the exit region, that is the region after the porous matrix, temperature ranges from 621K to 796K. It is worth seeing that the coldest place in this region is in its lower part. There was about a 273% temperature increase when comparing to the inlet air temperature of 293.15K.

## 7. REFERENCES

- Albanakis, C., Missirlis, D., Michailidis, N., Yakinthos, K., Goulas, A., Omar, H., Tspas, D., Granier, B., 2009. "Experimental analysis of the pressure drop and heat transfer through metal foams used as volumetric receivers under concentrated solar radiation". *Experimental Thermal and Fluid Science*, Vol. 33, pp. 246–252.
- Ávila-Marín, A. L., 2011. "Volumetric receivers in Solar Thermal Power Plants with Central Receiver System technology: A review". *Solar Energy*, Vol. 85, pp. 891–910.
- Behar, O.; Khellaf, A.; Mohammadi, K., 2013. "A Review of studies on central receiver solar thermal power Plants". *Renewable and Sustainable Energy Reviews*, Vol. 23, pp. 12–39.
- Buck, R., Brauning, T., Denk, T., Pfänder, M., Schwarzbozl, P., Tellez, F., 2002. Solar-Hybrid Gas Turbine-based Power Tower Systems (REFOS). In *Proceedings of the ASME 201 at Forum 2001, Solar Energy: The Power to Choose*, April 21–25, 2001, Washington, DC.
- Del Río, A., Korzynietzb, R., Briosoa, JA., Gallasa, M., Ordóñez, I., Queroa, M., and Díaza, C. "Soltrec - Pressurized volumetric solar air receiver technology"
- Hossain, M., Wilson, M., 2002. "Natural convection flow in a fluid-saturated porous medium enclosed by non-isothermal walls with heat generation". *International Journal of Thermal Sciences*, Vol. 41, pp. 447-454.
- Peter Heller a,\*, Markus Pfänder a, Thorsten Denk b, Felix Tellez c, Antonio Valverde b, Jesús Fernandez b, Arik Ring. Test and Evaluation of a Solar Powered Gas Turbine System.

## **8. RESPONSIBILITY NOTICE**

The authors are the only responsible for the printed material included in this paper.

## **9. ACKNOWLEDGEMENTS**

The authors thank FAPEMIG (Process: APQ-02457-12).